PCCP

Accepted Manuscript

ROYAL SOCIETY OF CHEMISTRY

rsc.li/pccp

View Article Online
DOI: 10.1039/C7CP07353D

Interfacial Electrostatics of Poly(vinylamine hydrochloride), Poly(diallyldimethylammonium chloride), Poly-L-lysine, and Poly-L-arginine Interacting with Lipid Bilayers

McGeachy, A. C.,[a] Dalchand, N.,[a] Caudill, E. R.,[b] Li, T.,[a] Doğangün, M.,[a] Olenick, L. L.,[a] Chang, H.,[a] Pedersen, J.A.,[b,c] Geiger, F.M.[a]

[a]Department of Chemistry, Northwestern University, 2145 Sheridan Road, Evanston, IL 60660

[b]Department of Chemistry and [c]Environmental Chemistry and Technology Program, University of Wisconsin-Madison, 680 North Park Street, Madison, WI 53706.

ABSTRACT. Charge densities of cationic polymers adsorbed to lipid bilayers are estimated from second harmonic generation (SHG) spectroscopy and quartz crystal microbalance with dissipation monitoring (QCM-D) measurements. The systems surveyed included poly(vinylamine hydrochloride) (PVAm), poly(diallyldimethylammonium chloride) (PDADMAC), poly-L-lysine (PLL), and poly-L-arginine (PLR), as well as polyalcohol controls. Upon accounting for the number of positive charges associated with each polyelectrolyte, the binding constants and apparent free energies of adsorption as estimated from SHG data are comparable despite differences in molecular masses and molecular structure, with ΔG_{ads} values of –61 ± 2, –58 ± 2, –56 ± 1,–52 ± 2, –52 ± 1 kJ/mol for $PDADMAC_{400}$, $PDADMAC_{100}$, PVAm, PLL, and PLR, respectively. Moreover, we find charge densities for polymer adlayers of approximately 0.3 C/m^2 for poly(diallyldimethylammonium chloride) while those of poly(vinylamine) hydrochloride, poly-L-lysine, and poly-L-arginine at approximately 0.2 C/m^2. Time-dependent studies indicate that polycation adsorption to supported lipid bilayers is only partially reversible for most of the polymers explored. Poly(diallyldimethylammonium chloride) does not demonstrate reversible binding even over long timescales (>8 hours).

View Article Online
DOI: 10.1039/C7CP07353D

I. Introduction. Widespread interest in and utility of antimicrobial polymers, cell-penetrating peptides, bioelectrodes, and biosensors has driven many experimental and theoretical studies devoted to elucidating the interactions of polymers and polycations with cell surfaces [1-7] and model systems.[6-17] Outstanding questions in this field pertain to surface charge and interfacial charge density,[4-6, 16, 18-19] particularly for polyelectrolytes in spherical nucleic acids,[20-22] antimicrobial surfaces,[4-5] nonviral vectors,[6] as well as films[23] and gels.[18] So far, experimental approaches providing answers to how many charges a polycation carries upon attachment to a surface or interface are scarce, if not absent, especially when considering those that require no external labels. Importantly, with reaction rates being proportional to absolute surface coverages, an accurate description of how polycations interact with surfaces or interfaces is also a key requirement for modeling their interaction kinetics. Examples are heterogeneous redox reactions and the heterogeneous kinetic salt effect:[24-25] in both cases the absolute number of charges on the adsorbed species needs to be known in order to predict the corresponding increases or decreases in the reaction rate depending on the ionic strength and charge state/speciation, the latter of which may change with ionic strength as well.[26-27]

Here, we argue that providing interfacial charge density estimates from experiments is important, as molecular dynamic (MD) simulations suggest that some linear polycations such as poly(vinylamine) and polyethylenimine (PEI) can accumulate, through electrostatic interactions, phosphatidylglycerol (PG) lipids present in simulated bacterial membranes,[28] a result also reported for polybetaines.[14] Poly(allylamine hydrochloride) (PAH) is another widely investigated polycation under exploration for use in thin films,[5, 29-31] drug delivery,[32] and cell encapsulation.[33] As a weak polyelectrolyte, PAH has been reported to shift its ammonium pK_a in multilayer films[23, 34-35] and at model biological interfaces,[36] a result not expected with polyelectrolytes

View Article Online
DOI: 10.1039/C7CP07353D

containing quaternary amines, such as poly(diallyldimethylammonium chloride). In addition to charge density, the structure of the charged functionality can significantly influence the interactions of the polymer with lipids and macromolecules and have biological consequences. For instance, atomistic simulations of PAH, PEI, poly(vinylamine), and poly-L-lysine (PLL) interactions with DNA reveal that two different binding behaviors that ultimately lead to the formation of polyplexes.[37] Of the polymers explored, only poly(vinylamine) embeds into the DNA major groove, a behavior not observed even with poly(allylamine) despite having similar functionalities. The authors hypothesized that the length of the pendant chains is responsible for this observation, as the amine group of poly(vinylamine) is one methylene shorter relative to poly(allylamine) (Figure 1). Further, in studies exploring the antimicrobial activity of copolymers with various cationic functional groups against *Escherichia coli*, polymers containing primary amines demonstrated a higher degree of antimicrobial activity relative to those bearing quaternary ammonium groups.[38]

With the importance of polyelectrolyte charge density in mind, we explore here the quantification of charge density and the ultimate role that charge density plays in the interactions that occur between polyelectrolytes having varying functionalization and supported lipid bilayers (SLBs) as models for biological membranes. To this end, we have recently published an approach to estimate charge density on adsorbed entities that pairs surface-sensitive nonlinear optical spectroscopies, namely second harmonic generation (SHG) and vibrational sum frequency generation (SFG) spectroscopies, with acoustic mass measurements from quartz crystal microbalance with dissipation monitoring (QCM-D) as well as coarse-grained and molecular dynamic simulations.[36] We are motivated by a previous study[39] exploring the role of chemical functionality, size, and charge in the disruption of SLBs, generation 7 (G7) amine-

View Article Online
DOI: 10.1039/C7CP07353D

terminated PAMAM dendrimers were shown to form and exacerbate membrane defects whereas this effect was reduced (G5) or eliminated (G3) in lower generation dendrimers. Moreover, replacing the terminal amine groups with acetamide, reduced the propensity even further for G5 dendrimers to produce holes in the SLB. While this study and others highlight the important role that size, charge, chemical functionality, and molecular mass can play in the interactions that they have model and actual cellular surfaces, they do not provide a quantitative measure for the surface charge of the dendrimers, SLB, or the adsorbed polymer layer. In a comparative study exploring the interactions of PLL and PLR nonamers with lipid bilayers composed from mixtures of anionic PG and zwitterionic phosphatidylcholine (PC) lipids, PLR was found to bind more favorably to lipid bilayers than PLL.[8] Although a pH-sensitive sensor composed of ortho-rhodamine B conjugated with the free amine of (1-hexadecanoyl-2-(9Z-octadecenoyl)-*sn*-glycero-3-phosphoethanolamine) was used to monitor changes in interfacial potential, no values for charge density or interfacial polymer concentration were reported due to stated limitations in the capabilities of the binding assay used.[8]

Our present work explores a suite of linear cationic polymers differing in chemical structures (Figure 1) that includes poly(vinylamine hydrochloride) (PVAm), poly(diallyldimethylammonium chloride) (PDADMAC), poly-L-lysine hydrobromide (PLL) and poly-L-arginine hydrochloride (PLR). This suite of polymers consists of various cationic groups including primary amines (PVAm and PLL), a quaternary ammonium (PDADMAC), and a guanidinium group (PLR). Given the diversity of the interactions that can occur between polycationic polymers, with varying chemical functionalities, [28, 40] and biological interfaces, this suite of polymers allows us to explore the applicability of our quantitative approach for estimating charge densities. Here, we use our label-free method for estimating polymer-bilayer

View Article Online
DOI: 10.1039/C7CP07353D

interactions to aid in the interpretation of such results and in understanding the molecular-level mechanisms by which polymers interact with biological surfaces. Specifically, we estimate interfacial charge densities from nonresonant second harmonic measurements that we pair with acoustic mass (polymer mass plus hydrodynamically coupled water) estimates from QCM-D measurements. This approach provides the lower bounds of charge per attached polycation, because (1) not all charges associated with the polycation may be located within the SHG active interfacial region and (2) the water content contributing to the mass estimates is not known quantitatively unless another technique such as nanoplasmonic sensing or optical waveguide lightmode spectroscopy is used, which is not the case here.

II. Experimental Methods.

A. Laser System. SHG spectroscopy measurements were conducted with the output from a Ti:sapphire laser system (Hurricane, Spectra-Physics, 800 nm, 120 fs pulses at a repetition rate of 80 MHz). The power is attenuated using a variable density filter down to 0.50 ± 0.01 W, and the beam is directed through a longpass filter to remove residual 400 nm light from the oscillator. The output beam from the oscillator is split, and part of the beam is used to continuously monitor the power over the course of the experiment using a power meter (Newport 1917-R) to correct the SHG signal for any drifts in power. The transmitted 800 nm beam is focused on the fused silica/water interface at an incident angle of 60° from the surface normal, less than the angle of total internal reflection. The fundamental 800 nm light is recollimated and then filtered using a 400 nm bandpass filter (FBH400-40M ThorLabs, >90% peak transmission) and a monochromator tuned to the SHG wavelength (400 nm), as described earlier.[41] The SHG light is then directed into a photomultiplier tube where the signal is amplified and collected by a gated photon counter (Stanford Research Systems). The polarization combination used in *s*-in/all out.

View Article Online
DOI: 10.1039/C7CP07353D

B. Sample Cell and Flow System. SHG spectroscopy flow experiments were carried out using a home-built Teflon flow-cell and a fused silica hemispherical lens (ISP Optics, 1-in diameter, QU-HS-25-1) that has been previously described.[36, 42-44] Our Teflon flow-cell, three-way valve, and all connected components, including tubing (PTFE tube (1/16") and Swagelock fittings, were sonicated in methanol (~30 min) prior to each experiment. The flow-cell was then dried under nitrogen and oxygen plasma cleaned (Harrick Plasma Cleaner, 18W, 300-500 mTorr) for 10 minutes. Prior to use, the tubing was flushed with Tris buffer solution. The PTFE-tubing was changed frequently to avoid contamination and cleaned with methanol, Millipore water (>18 MΩ), and buffer before reuse.

Hemispherical lenses were cleaned with Nochromix® for at least 1 hour and then rinsed with Millipore water. The hemispherical lenses were then transferred to a beaker containing fresh methanol and sonicated for ten minutes, rinsed with Millipore water, and dried under N_2. Lastly, the hemispherical lenses were plasma cleaned for 10 minutes.

C. Buffer, Vesicle, and Polymer Preparation. Sodium chloride (NaCl, Alfa Aesar, >99%), Trizma base (Tris, Sigma Aldrich), calcium chloride dihydrate ($CaCl_2$ $2H_2O$, Sigma Aldrich) and Millipore water were used for buffer preparation. All buffer solutions were adjusted to a pH of 7.4 using dilute solutions of sodium hydroxide and hydrochloric acid, as necessary. Two-milligram vesicle suspensions of 9:1 molar ratios of 1,2-dimyristoyl-*sn*-glycero-3-phosphocholine (DMPC, Avanti Polar Lipids) and 1,2-dimyristoyl-*sn*-glycero-3-phosphorylglycerol sodium salt (DMPG, Avanti Polar Lipids) were dried under a gentle stream of N_2 and placed in a vacuum desiccator for at least 3 hours. As multiple methods for reconstituting and forming supported lipid bilayers exist, we used two methods somewhat interchangeably in order to evaluate the reproducibility and transferability of the results that we

View Article Online
DOI: 10.1039/C7CP07353D

observe in our SHG measurements. To assess whether the choice of method of vesicle preparation impacted our results, we conducted SHG measurements using both lipid vesicle preparation methods. These methods and experiments are further discussed in the Supporting Information. The concentration of Tris buffer (0.01 M) adjusted to pH 7.4 is constant throughout and henceforth will be omitted. The bilayers prepared are well formed, as characterized in detail in our previous reports.[42, 45]

Poly(diallyldimethylammonium chloride) (PDADMAC, 400-500 kDa, 20 % wt. in H_2O), poly-L-lysine hydrobromide (PLL, 4-15 kDa), and poly-L-arginine hydrochloride (PLR, 5-15 kDa) were purchased from Sigma Aldrich and used without further purification. Poly(vinylamine hydrochloride (PVAm, 25 kDa) was purchased from Polysciences and used without further purification. All polymer solutions, with the exception of PDADMAC, were prepared and stored in 0.001 M NaCl. Control experiments described in the Supporting Information were also performed with poly(vinyl alcohol) with molecular weights of 9 kDa (Product Number 360627) and 85 kDa (Product Number 363081) (PVA), and poly(acrylic acid) (PAA, Product Number 416037) were also purchased from Sigma Aldrich. Polymer concentrations were determined based on the average molecular mass of the polymer, and the average number of repeat units was determined by dividing the average polymer molecular mass by the molar mass of one monomer, including the counterion mass.

D. SHG Adsorption Experiments. The flow cell was equilibrated with 0.1 M NaCl buffer (Method 1) or 0.15 M NaCl and 0.005 M $CaCl_2$ (Method 2), and the SHG signal was monitored for at least 10 minutes to obtain a stable baseline. Vesicle-containing solutions were then introduced into the Teflon flow cell *via* the three-way valve at a rate of approximately 2 mL/min. Supported lipid bilayers formed over the course of at least 15 minutes *via* the vesicle fusion

View Article Online
DOI: 10.1039/C7CP07353D

method.[36, 42, 46] The resulting 9:1 DMPC/DMPG bilayer was then rinsed at the same flow rate with (1) 20 mL of 0.1 M NaCl buffer (Method 1) or (2) 10 mL of 0.15 M NaCl and 0.005 M $CaCl_2$ buffer, 10 mL of 0.15 M NaCl buffer, and 20 mL of 0.1 M NaCl buffer (Method 2) to remove any excess vesicles, and the SHG signal was monitored for at least 20 minutes or until stable. The SHG signal recorded prior to polymer solution introduction serves as the baseline signal to which the data are normalized. To generate SHG adsorption isotherms, sequentially higher concentrations of polymer were introduced into the flow cell (20 mL at 2 mL/min), and the SHG signal was allowed to stabilize (~30 minutes). The average SHG signal over the last 10-15 minutes was used.

Single-exposure experiments were also performed to assess reversibility. In these single exposure experiments, referred to herein as on/off experiments, the SHG baseline signal from a supported lipid bilayer formed from 9:1 DMPC/DMPG at 0.1 M NaCl was collected for at least ~45 minutes. Then, 20 mL of solution at the desired polymer concentration was introduced into the flow cell, maintaining the same background electrolyte concentration (0.1 M NaCl), and the SHG signal was monitored for 70 minutes before rinsing with 20 mL of a polymer-free solution at 0.1 M NaCl. In experiments conducted at lower ionic strengths (0.01 M), where the only contribution to ionic strength was the Tris buffer (i.e., no added NaCl), the initial rinse with 0.1 M NaCl after bilayer formation, was followed by a rinse with 20 mL 0.01 M Tris buffer (no NaCl present). The adsorption isotherms and on/off experiments were then carried out in the same manner using salt-free buffer. All experiments were carried out at room temperature (20-21°C) which is just below the temperature at which the lipids transition from an ordered gel phase to a disordered liquid crystalline phase of DMPC and DMPG (T_m 24 and 23°C respectively).

View Article Online
DOI: 10.1039/C7CP07353D

E. SHG Theory and Modeling Interfacial Adsorption Processes. As described extensively in the literature, second harmonic generation $\chi^{(3)}$ measurements can provide useful information about binding thermodynamics and electrostatics.[36, 41, 47-49] The SHG signal intensity from charged interfaces is directly proportional to the electric field generated at the second harmonic as shown in Equation 1, written for the conditions of total our ionic strength (0.1 M) employed here, where phase matching is not important:

$$I_{SHG} \propto |E_{SHG}|^2 \propto |\chi^{(2)} E_\omega E_\omega + \chi^{(3)} E_\omega E_\omega \Phi_0|^2 \quad 1$$

Here, $\chi^{(2)}$ and $\chi^{(3)}$are the second- and third-order nonlinear susceptibility tensors, $E_\omega$is the incident electric field oscillating at the fundamental frequency (800 nm), and Φ_0 is the interfacial potential,[47, 50-52] again written for ionic strength conditions for which phase matching is not important (I=0.1 M) in our reflection geometry[49]

$$E_{SHG} \propto A + B\Phi_0 \quad 2$$

As shown in Equations 1 and 2, the electric field generated at the second harmonic (E_{SHG}) is proportional to the interfacial potential, Φ_0, where A and B are constants specific to the system that contain the second- and third-order nonlinear susceptibility tensors, respectively) and the incident electric field oscillating at 800 nm, as described above and further explained elsewhere.[36]

Combining surface complexation models (i.e., Gouy-Chapman or triple layer)[53-54] and adsorption models like the Langmuir or Hill isotherms (*vide infra*) allows us to quantify the interactions between the polyelectrolytes and the supported lipid bilayers under investigation in this work. Specifically, the approach enables us to estimate charge densities, equilibrium constants, and ultimately the free energies of adsorption. Recently, the Hill adsorption model was applied to the adsorption of PLL and PLR to lipid bilayers formed from 1-palmitoyl-2-oleoyl-*sn*-glycero-3-

View Article Online
DOI: 10.1039/C7CP07353D

phospho-(1'*rac*-glycerol) (sodium salt) (POPG) and 1-palmitoyl-2-oleoyl-*sn*-glycero-3-phosphocholine (POPC).[8] As reported by Cremer and co-workers, using a simple Langmuir model to describe the adsorption of PLL and PLR to SLBs is difficult. These studies revealed that PLR nonamers adsorbed more cooperatively to SLBs than did PLL nonamers, although binding of PLR and PLL was largely anti-cooperative under most conditions explored.[8] Given that some cooperative binding is expected in the adsorption of PLL and PLR specifically in these systems, we opted to use the Hill model, which provides better fits with the experimental data presented here. A comparison of the results derived from combinations of two surface complexation models (Triple-Layer and Gouy-Chapman), and Langmuir and Hill models is provided in the Supporting Information.

The Langmuir adsorption model describes the adsorption of a species to a homogeneous, flat surface.[55-56] Additionally, it assumes that lateral interactions between adsorbed species occupying adjacent sites do not occur and that all binding sites are equivalent. The model takes the form of $\theta = \frac{K_{ads}M}{1+K_{ads}M}$ where θ represents the fractional surface coverage, K_{ads} is the apparent equilibrium constant of polymer adsorption, and M is the bulk polymer concentration. In an extension of the Langmuir model, the Hill model[57] accounts for intramolecular coupling (i.e. change in binding affinity at one site in response to binding at another site). The Hill model takes the form $\theta = \frac{K_{ads}^{n}M^{n}}{1+K_{ads}^{n}M^{n}]}$.[57-58] The Hill-coefficient, *n,* describes cooperativity. If $n > 1$, the adsorption process is cooperative and as the concentration of adsorbate increases, the binding affinity increases. Conversely, when $n < 1$, the process is typically described as being anti-cooperative, and increasing adsorbate concentrations at the interface reduces the binding affinity. However, we caution that the interpretation of cooperativity solely based on the experimentally determined Hill coefficient is problematic. For example, adsorption to heterogeneous surfaces

View Article Online
DOI: 10.1039/C7CP07353D

can also result in artificially low n values[59-60] while electrostatics and reductions in dimensionality can explain high values for n.[58]

Combining Equation 2 with the Gouy-Chapman and Hill equations, we arrive at Equation 3:

$$E_{SHG} \propto A + B \sinh^{-1}\left(\left(\sigma_0 + \sigma_{ads}\left(\frac{K_{ads}^n M^n}{1 + K_{ads}^n M^n}\right)\right)\left(\frac{8.44\, M^{1/2} m^2 C^{-1}}{\sqrt{M + C_{elec}}}\right)\right) \quad 3$$

where $\sigma_0$is the charge density of the 9:1 DMPC/DMPG bilayer, σ_{ads} is the charge density of the adsorbed polymer (adlayer) at monolayer coverage, K_{ads} is the apparent equilibrium constant of polymer adsorption in liters per mole, n is the Hill coefficient (for the Langmuir model n = 1) which describes the cooperativity of the adsorption process, M is the bulk polymer concentration in moles per liter, and C_{elec} is the background electrolyte concentration (0.1 M NaCl plus 0.008 M contribution from Tris) in moles per liter.

F. QCM-D Sensor Preparation and SLB Formation. Our QCM-D sensor preparation, instrumental details, and methods for forming supported lipid bilayers has been described previously. Briefly, the SiO_2-coated QCM-D sensors (QSX303, Biolin Scientific) were rinsed with ethanol and copious amounts of ultrapure water (18 MΩ·cm; Barnstead NANOPure). The sensors were then dried under a stream of N_2 and plasma cleaned in a UV/Ozone chamber (Prochamber, Bioforce Nanosciences) for 20 minutes before being installed in the flow cell.

Vesicles used in these studies were prepared using Method 2 for all of the polymers explored herein. Supported lipid bilayers were formed in a Q-Sense E4 QCM-D instrument that contains four SiO_2 sensors mounted in a flow module (QFM 401) allowing for up to four simultaneous measurements to be performed in parallel. QCM-D sensors were first equilibrated with 0.1 M NaCl, 0.01 M Tris, 0.005 M $CaCl_2$ buffer until the baseline stabilized. A flow rate of 100 μL/min was maintained throughout the experiment. Lipid suspensions were introduced into the flow

View Article Online
DOI: 10.1039/C7CP07353D

chamber for 15 minutes. Then, the flow cell was flushed with vesicle-free 0.1 M NaCl, 0.01 M Tris, 0.005 M $CaCl_2$. When the solution was switched to 0.1 M NaCl, 0.01 M Tris, bilayer formation occurred. The flow cell was rinsed for at least 10 additional minutes following this occurrence until Δ*frequency* (Δ*f*) and Δ*dissipation* (Δ*D*) traces were stabilized. The solution at the desired polymer concentration was then flowed over the bilayer until the signal plateaued for at least 10 minutes. To assess reversibility, 0.1 M NaCl polymer-free buffer solutions were introduced for at least 20 minutes. Bilayers were formed at 23 ± 0.5 °C, and the flow cells were maintained at this temperature for the entirety of the experiments. A brief theoretical background on QCM-D along with a discussion of the methods employed to analyze QCM-D data is provided in the accompanying Supporting Information.

III. Results and Discussion.

A. Polycation Adsorption to Supported Lipid Bilayers. The adsorption of polycationic polymers to membranes is driven, in part, by short-range electrostatic interactions, although some studies have suggested that hydrophobic interactions and hydrogen bonding are also important in these interactions.[28, 61] While PLR and PVAm adsorb to lipid bilayers formed from pure zwitterionic DMPC and a 9:1 mixture of DMPC/DMPG, as evidenced by the decrease in SHG signal upon introduction of polymer solution, PLL and PDADMAC do not change the observed SHG signal considerably upon interaction with SLBs formed from DMPC (Figure 2). These results suggest that, as expected, PLL and PLR adsorption to SLBs containing PG-lipids is driven, at least in part, by electrostatics. These qualitative outcomes are similar to what has been reported elsewhere.[8, 62]

B. Reversibility and Timescales. SHG and QCM-D were also used to investigate the reversibility of polycation binding to the SLBs. In these experiments, SLBs were exposed to 50

View Article Online
DOI: 10.1039/C7CP07353D

nM concentrations of PVAm or PDADMAC or to 0.5 μM of PLL or PLR, at 0.1 M NaCl. These polymer concentrations correspond to saturation coverage as determined by SHG, as discussed later from our adsorption isotherm measurements.

PLL, PLR, and PVAm interacting with SLBs formed from 9:1 DMPC/DMPG all show partial to complete reversibility upon rinsing with 0.1 M NaCl polymer-free buffer solutions (Figure 2B), albeit over long timescales (>8 hours). PLL, PLR, and PVAm interacting with SLBs formed from 9:1 DMPC/DMPG all show partial to complete reversibility upon rinsing with 0.1 M NaCl polymer-free buffer solutions (Figure 2B), albeit over long timescales (>8 hours). We note here that such long timescales are generally not probed using nonlinear optics or quartz crystal microbalances, as drifts in the signal due to a variety of exogenous signal variations typically prevent one from making such "long-term" measurements. Indeed, Fig. 2B shows that had the measurements ceased after two hours, already an impressive feat in probing surface processes at buried interfaces using ultrafast lasers, the varying extent of reversible binding for PVAm, PLR, PLL, and $PDADMAC_{100}$ would not have been identified. An important part to overcoming the difficulty of long-term surface interaction tracking is due to the low long-term drift of our Ti:S oscillator (0.5% drift in power over two hours, as described in Troiano et al.)[32]

PDADMAC, regardless of molecular mass, remains adsorbed to the SLB surface as evidenced by the continued suppression of the SHG signal after rinsing, as compared to the SHG signal of the bare SLB prior to exposure. These results might be explained by the significantly larger molecular mass of the PDADMAC polymers, as compared to the (reversibly bound) much lower molecular mass polymers (PVAm, PLL, and PLR). While QCM-D reversibility studies do not indicate that the adsorption process demonstrates reversibility over 20 minutes of rinsing, the longer-term SHG studies indicate that polymer adsorption is indeed reversible over longer

View Article Online
DOI: 10.1039/C7CP07353D

timescales (>8 hours). Indeed, close to full reversibility is observed in the case of PVAm over these timescales. We therefore apply Langmuir model-based adsorption isotherms to describe the adsorption behavior of the various polyelectrolytes studied herein.

Note that neither SHG spectroscopy nor QCM-D can independently distinguish between removal of lipids, polymer, or a combination thereof. However, vibrational sum frequency generation (SFG) spectroscopy experiments show only negligible changes in the spectral features from the SLBs studied here before and after they have been exposed to the polycations (Supporting Information). These results indicate that the bilayers are largely preserved under the conditions of our experiments.

C. Comparable Binding Free Energies Across All Polymers Despite Differences in Molecular Structure and Mass. Using our previously published approach,[36] which is described in detail in Section II.E. and the Supporting Information, we estimated charge densities, equilibrium constants, mass uptake, degree of ionization, and free energies of adsorption for the polycation/bilayer systems studied in this work (Table 1). Figure 3A shows that with increasing polymer concentration the SHG signal intensity decreases as the bilayer surface charge decreases in magnitude due to polycation attachment. Control SHG experiments using (uncharged) polyalcohols show negligible binding ("PVOH" in Figure 3A).

Dividing the average molecular mass of the polymer by the molar mass of the corresponding monomer (including the mass contributions from the counterion), we now account for molar mass differences across the various polycations we studied (Figure 3B). Plotting the SHG response after normalizing it to the zero-polycation concentration case and referencing to the response obtained for the highest polycation concentration reveals that the individual adsorption isotherms of all the polycations converge on a single curve, with an inflection point

View Article Online
DOI: 10.1039/C7CP07353D

corresponding to 10^{-6} mol/L of cations in solution (Figure 3C). Our approach is similar to an exploration of the binding activity of polycations with pendent biguanide or quaternary ammonium functional groups,[1-2] in which accounting for molecular mass differences between the two polymers led to comparable antimicrobial activity.

As described in the Section II.E, we apply a combined Gouy-Chapman and Hill model to describe the binding of these polymers to the bilayer surface. When referenced to the molarity of water (55.5 M), the apparent equilibrium constants determined from SHG isotherms correspond to apparent adsorption free energies of –61 ± 2, –58 ± 2, –57 ± 1,–52 ± 2, –52 ± 1 kJ/mol for $PDADMAC_{400}$, $PDADMAC_{100}$, PVAm, PLL, and PLR, respectively (Table 1). Comparable free energies associated with the adsorption of PDADMAC to that of the polymers explored herein are somewhat surprising since PDADMAC is expected to only weakly interact with lipids, given the charge shielding in the quaternary ammonium groups. The nuances of the binding behavior of the polycations studied are likely to manifest themselves in their binding entropies and enthalpies. However, temperature-dependent studies were not carried out in this present work. For instance, given differences in the molecular weights and the differing propensities of the polycations described here to reorient or release water and counterions from the bilayer surface upon adsorption, and to perturb local lipid ordering,[28] it is conceivable that the entropic contributions to the free energies vary significantly across polymers. Future experiments will address this point through the use of temperature-controlled experiments, an aim beyond the scope of this current work.

In addition to providing estimates for charge densities, the approach described herein also allows us to explore the cooperative nature, or the lack thereof, of polyelectrolyte adsorption to lipid bilayers. Atomistic-scale MD simulations suggest that strong interactions between PVAm and

View Article Online
DOI: 10.1039/C7CP07353D

the headgroups of PG-lipids results in competitive binding between two different PVAm polymer chains.[28] With a Hill coefficient of 3, we find that the adsorption of PVAm to 9:1 DMPC/DMPG bilayers is more positively cooperative than any of the other polymers explored herein. In fact, none of the other polymers demonstrate positive or negative cooperativity based on their estimated Hill coefficients, which are close to unity. Unlike PLL and PLR, two other relatively weak polyelectrolytes, PVAm is subject to the polyelectrolyte effect. Specifically, the relative distance between neighboring amine groups gives rise to a unique ionization behavior that allows PVAm to maintain partially ionization over most of the pH scale.[63] Our previous report on PAH showed that the pK_a shift associated with PAH adsorption to 9:1 DMPC/DMPG could be substantial.[36] Here, we expect this shift to be even larger given the unique relationship between neighboring amine groups associated with PVAm.

D. Charge Densities of Polycations Attached to SLBs. Previous work indicates that SLBs formed from 9:1 mixtures of DMPC and DMPG are associated with a negative charge density (-0.11 ± 0.06 C/m^2).[36] Accounting for this charge density, and using equation 3, we estimate the total interfacial charge densities listed in Table I. Specifically, the charge densities reported in Table 1 are the charge densities for the adlayers after accounting for the charge density of the SLB (σ_{ads} in Equation 3). PDADMAC (Figure 4A, 4B) and PLR (Figure 4e) appear to bind to a large extent, reversing the surface charge of the lipid bilayer. Unfortunately, considerably large errors on the estimated charge densities of PLL (Figure 4D) and PVAm (Figure 4C) prevent us from drawing further conclusions on whether adsorption to SLBs formed from 9:1 DMPC/DMPG results merely in charge neutralization or if charge is indeed reversed. These results are in line, at least in part, with previously published studies employing atomistic-level MD simulations which show that some polycations neutralize or cause overcharging of lipid

View Article Online
DOI: 10.1039/C7CP07353D

bilayers composed from 4:1 mixtures of PE/PG.[28] In these simulations, accumulation of chloride ions at the Helmholtz plane suggests that PVA, PEI, and PLL overcharge the membrane surface upon adsorption. Further, adsorption of PVAm to PG-containing phospholipid bilayers can (1) cooperatively accumulate Na^+ ions and (2) induce the reorientation of water molecules at the membrane surface.[28]

As stated in Section II.E, we assume that $\chi^{(3)}$, which accounts for the net orientation of water molecules polarized due to the presence of a charged interface, remains constant over the course of our experiments. Given that SHG signal intensity is proportional to the square modulus of the SHG *E*-field, and the number of water molecules present remains constant throughout, the reorientation of water molecules upon interfacial overcharging is not captured in these measurements. Ongoing experiments in this area that focus on the O–H stretching vibrations using SFG spectroscopy will be reported in due course.

As a complement to the charge densities, and to provide additional insight into the adsorption properties of the polycations explored herein, QCM-D experiments were conducted under the same experimental conditions (0.1 M NaCl, 0.01 M Tris buffer, pH 7.4). QCM-D mass measurements yield the acoustic mass associated with polymer adsorption (which contains hydrodynamically coupled solvent) to SLBs from which we estimate the number density of polymer chains associated with the bilayer and the degree of ionization. Using the acoustic mass data from QCM-D measurements, and assuming that 30% of the sensed mass adsorbed is due to mass contributions from coupled water molecules,[64] we estimate number densities (in terms of polymer density per square centimeter) on the order of 10^{11}-10^{13} polymers/cm^2 corresponding to approximately 10^{14} charges/cm^2 (Table I), again given the caveat that not all charges associated with the adsorbed polycations may be captured in the SHG-active interfacial region. Previous

View Article Online
DOI: 10.1039/C7CP07353D

studies using colorimetric assays have reported a minimum surface charge density on the order of 10^{15}-10^{16} positive charges per square centimeter required for effective antibacterial activity.[4] Here, our adsorbed film charge densities are just below those values.

Combining the charge densities from our SHG experiments with the estimates for polymer mass density from the QCM-D measurements, and assuming again that ~30% of the associated mass is attributed to water molecules associated with the adsorbed polymer, we find that 7%, 20%, 30% of the ionizable groups of PVAm, PLL, and PLR are charged, respectively, under the conditions of our experiments, provided that each amine group is available to participate in binding to the membrane surface and is sensed in the SHG active interfacial region. These results show that PVAm is associated with the lowest degree of ionization of any of the polymers explored herein. At pH 7.4, PVAm is expected to be approximately 50-70% ionized[65] but ionization depends strongly on the extent of hydrolysis.[66] Given the previously discussed caveats, and the uncertainty in the percent of acoustic mass attributable to polymer alone (i.e. excluding contributions from hydryodynamically coupled water molecules), we have also provided estimates for percent ionization and polymer number density with water contents ranging from 1-70% of the acoustic mass. (Supporting Information)

In addition to the result regarding PVAm discussed above, PDADMAC also appears to have a smaller fraction of charged groups than expected. This result is consistent with reports that polymers containing quaternary ammonium functional groups interact only weakly with lipid membranes[40] and points towards the special role that contact ion pairing, or counter ion condensation, may play in this case.

IV. Conclusions.

View Article Online
DOI: 10.1039/C7CP07353D

Polyelectrolyte charge density is thought to be critically important for the function of many engineered and naturally occurring systems, including spherical nucleic acids, antimicrobial surfaces, nonviral vectors, and in the formation of films and gels. However, concrete – as opposed to hypothetical – interfacial charge density data have been difficult to obtain, largely because of a lack of label-free, surface specific measurement techniques that can provide electrostatic information at buried aqueous/solid interfaces. As an important first step towards understanding how charge density correlates to the formation of these complex assemblies, we have presented here an experimental tool that pairs quartz crystal microbalance with dissipation (QCM-D) monitoring with nonlinear optical spectroscopy, specifically, second harmonic generation (SHG) that is used to estimate the charge densities of the adsorbed layers formed on supported lipid bilayers. These studies are important not only for the study of the interactions of polyelectrolytes and model membranes but also in the study of similarly formed thin films and polymer-cushioned SLBs.[67-71]

Using surface charge densities the determined using the SHG Eisenthal $\chi^{(3)}$ method and the attached mass from the QCM-D experiments, we estimate the number of charges associated with a polyelectrolyte attached to a lipid bilayer. These polyelectrolytes include poly(vinylamine hydrochloride), poly(diallyldimethylammonium chloride), poly-L-lysine hydrobromide, and poly-L-arginine hydrochloride. Through these studies, we have begun to explore a structure-charge density relationship that compares the various polycations and their subsequent interactions with idealized model bilayers. We find that upon accounting for the number of positive charges associated with each polyelectrolyte, the free energies of adsorption are comparable despite differences in molecular masses and functionalities. Further, these results provide information regarding the role of electrostatics in these interactions, but also indicates

View Article Online
DOI: 10.1039/C7CP07353D

that other interactions are important to polyelectrolyte/membrane interactions. Future work will focus on more tunable polyelectrolytes that can be systematically structurally altered to yield better control over the number of associated positive charges.

Acknowledgements. This work is supported by the National Science Foundation under the Center for Sustainable Nanotechnology, Grant No.CHE-1503408. ACM gratefully acknowledges support from the U.S. National Science Foundation Graduate Research Fellowship Program. JAP gratefully acknowledges support from the William Rothermel-Bascom Professorship. FMG gratefully acknowledges support from a Friedrich Wilhelm Bessel Prize from the Alexander von Humboldt Foundation.

View Article Online
DOI: 10.1039/C7CP07353D

References.

1. Ikeda, T.; Yamaguchi, H.; Tazuke, S., New Polymeric Biocides - Synthesis and Antibacterial Activities of Polycations with Pendant Biguanide Groups. *Antimicrob. Agents Chemother.* **1984**, *26*, 139-144.
2. Ikeda, T.; Hirayama, H.; Yamaguchi, H.; Tazuke, S.; Watanabe, M., Polycationic Biocides with Pendant Active Groups - Molecular-Weight Dependence of Antibacterial Activity. *Antimicrob. Agents Chemother.* **1986**, *30*, 132-136.
3. Zhang, C.; Ying, Z. M.; Luo, Q. J.; Du, H.; Wang, Y.; Zhang, K.; Yan, S. G.; Li, X. D.; Shen, Z. Q.; Zhu, W. P., Poly(Hexamethylene Guanidine)-Based Hydrogels with Long Lasting Antimicrobial Activity and Low Toxicity. *J. Polym. Sci. Pol. Chem.* **2017**, *55*, 2027-2035.
4. Kugler, R.; Bouloussa, O.; Rondelez, F., Evidence of a Charge-Density Threshold for Optimum Efficiency of Biocidal Cationic Surfaces. *Microbiology-(UK)* **2005**, *151*, 1341-1348.
5. Iarikov, D. D.; Kargar, M.; Sahari, A.; Russel, L.; Gause, K. T.; Behkam, B.; Ducker, W. A., Antimicrobial Surfaces Using Covalently Bound Polyallylamine. *Biomacromolecules* **2014**, *15*, 169-176.
6. Vaidyanathan, S.; Orr, B. G.; Holl, M. M. B., Role of Cell Membrane Vector Interactions in Successful Gene Delivery. *Accounts of Chemical Research* **2016**, *49*, 1486-1493.
7. Kiss, E., et al., Membrane Affinity and Antibacterial Properties of Cationic Polyelectrolytes with Different Hydrophobicity. *Macromol. Biosci.* **2012**, *12*, 1181-1189.
8. Robison, A. D.; Sun, S.; Poyton, M. F.; Johnson, G. A.; Pellois, J. P.; Jungwirth, P.; Vazdar, M.; Cremer, P. S., Polyarginine Interacts More Strongly and Cooperatively Than Polylysine with Phospholipid Bilayers. *Journal of Physical Chemistry B* **2016**, *120*, 9287-9296.
9. Mertins, O.; Dimova, R., Insights on the Interactions of Chitosan with Phospholipid Vesicles. Part Ii: Membrane Stiffening and Pore Formation. *Langmuir* **2013**, *29*, 14552-14559.
10. Yaroslavov, A. A.; Yaroslavova, E. G.; Rakhnyanskaya, A. A.; Menger, F. M.; Kabanov, V. A., Modulation of Interaction of Polycations with Negative Unilamellar Lipid Vesicles. *Colloids and Surfaces B-Biointerfaces* **1999**, *16*, 29-43.
11. Yaroslavov, A. A.; Kuchenkova, O. Y.; Okuneva, I. B.; Melik-Nubarov, N. S.; Kozlova, N. O.; Lobyshev, V. I.; Menger, F. M.; Kabanov, V. A., Effect of Polylysine on Transformations and Permeability of Negative Vesicular Membranes. *Biochimica Et Biophysica Acta-Biomembranes* **2003**, *1611*, 44-54.
12. Alliband, A.; Meece, F. A.; Jayasinghe, C.; Burns, D. H., Synthesis and Characterization of Picket Porphyrin Receptors That Bind Phosphatidylglycerol, an Anionic Phospholipid Found in Bacterial Membranes. *Journal of Organic Chemistry* **2013**, *78*, 356-362.
13. Takechi, Y.; Tanaka, H.; Kitayama, H.; Yoshii, H.; Tanaka, M.; Saito, H., Comparative Study on the Interaction of Cell-Penetrating Polycationic Polymers with Lipid Membranes. *Chemistry and Physics of Lipids* **2012**, *165*, 51-58.
14. Yaroslavov, A. A.; Sitnikova, T. A.; Rakhnyanskaya, A. A.; Yaroslavova, E. G.; Davydov, D. A.; Burova, T. V.; Grinberg, V. Y.; Shi, L.; Menger, F. M., Biomembrane Sensitivity to Structural Changes in Bound Polymers. *Journal of the American Chemical Society* **2009**, *131*, 1666-+.
15. Kreuzer, M.; Trapp, M.; Dahint, R.; Steitz, R., Polymer-Induced Swelling of Solid-Supported Lipid Membranes. *Membranes* **2016**, *6*, 15.
16. Yaroslavov, A. A.; Melik-Nubarov, N. S.; Menger, F. M., Polymer-Induced Flip-Flop in Biomembranes. *Accounts of Chemical Research* **2006**, *39*, 702-710.

View Article Online
DOI: 10.1039/C7CP07353D

17. Xie, A. F.; Granick, S., Phospholipid Membranes as Substrates for Polymer Adsorption. *Nature Materials* **2002**, *1*, 129-133.
18. Zhou, S.; Burger, C.; Yeh, F.; Chu, B., Charge Density Effect of Polyelectrolyte Chains on the Nanostructures of Polyelectrolyte−Surfactant Complexes. *Macromolecules* **1998**, *31*, 8157-8163.
19. de Meijere, K.; Brezesinski, G.; Pfohl, T.; Mohwald, H., Influence of the Polymer Charge Density on Lipid-Polyelectrolyte Complexes at the Air/Water Interface. *Journal of Physical Chemistry B* **1999**, *103*, 8888-8893.
20. Banga, R. J.; Chernyak, N.; Narayan, S. P.; Nguyen, S. T.; Mirkin, C. A., Liposomal Spherical Nucleic Acids. *Journal of the American Chemical Society* **2014**, *136*, 9866-9869.
21. Chinen, A. B.; Ferrer, J. R.; Merkel, T. J.; Mirkin, C. A., Relationships between Poly(Ethylene Glycol) Modifications on Rna-Spherical Nucleic Acid Conjugates and Cellular Uptake and Circulation Time. *Bioconjugate Chemistry* **2016**, *27*, 2715-2721.
22. Cutler, J. I.; Auyeung, E.; Mirkin, C. A., Spherical Nucleic Acids. *Journal of the American Chemical Society* **2012**, *134*, 1376-1391.
23. Choi, J.; Rubner, M. F., Influence of the Degree of Ionization on Weak Polyelectrolyte Multilayer Assembly. *Macromolecules* **2005**, *38*, 116-124.
24. Gibbs-Davis, J. M.; Kruk, J. J.; Konek, C. T.; Scheidt, K. A.; Geiger, F. M., Jammed Acid-Base Chemistry at Interfaces. *J. Am. Chem. Soc.* **2008**, *130*, 15444-15447.
25. Atkins, P.; de Paula, J., *Atkins' Physical Chemistry*; OUP Oxford, 2010.
26. Jordan, D. S.; Saslow, S. A.; Geiger, F. M., Exponential Sensitivity and Speciation of Al(Iii), Sc(Iii), Y(Iii), La(Iii), and Gd(Iii) at Fused Silica/Water Interfaces". *J. Phys. Chem. A* **2011**, *115*, 14438-14445.
27. Malin, J. N.; Holland, J. G.; Geiger, F. M., Free Energy Relationships in the Electric Double Layer and Alkali Earth Speciation at the Fused Silica/Water Interface. *J. Phys. Chem. C* **2009**, *113*.
28. Kostritskii, A. Y.; Kondinskaia, D. A.; Nesterenko, A. M.; Gurtovenko, A. A., Adsorption of Synthetic Cationic Polymers on Model Phospholipid Membranes: Insight from Atomic-Scale Molecular Dynamics Simulations. *Langmuir* **2016**, *32*, 10402-10414.
29. Petrov, A. I.; Antipov, A. A.; Sukhorukov, G. B., Base-Acid Equilibria in Polyelectrolyte Systems: From Weak Polvelectrolytes to Interpolyelectrolyte Complexes and Multilayered Polyelectrolyte Shells. *Macromolecules* **2003**, *36*, 10079-10086.
30. Parveen, N.; Schonhoff, M., Quantifying and Controlling the Cation Uptake Upon Hydrated Ionic Liquid-Induced Swelling of Polyelectrolyte Multilayers. *Soft Matter* **2017**, *13*, 1988-1997.
31. Kovtyukhova, N. I.; Ollivier, P. J.; Martin, B. R.; Mallouk, T. E.; Chizhik, S. A.; Buzaneva, E. V.; Gorchinskiy, A. D., Layer-by-Layer Assembly of Ultrathin Composite Films from Micron-Sized Graphite Oxide Sheets and Polycations. *Chemistry of Materials* **1999**, *11*, 771-778.
32. Chung, A. J.; Rubner, M. F., Methods of Loading and Releasing Low Molecular Weight Cationic Molecules in Weak Polyelectrolyte Multilayer Films. *Langmuir* **2002**, *18*, 1176-1183.
33. Wang, B.; Zhang, Y. Y.; Mao, Z. W.; Gao, C. Y., Cellular Uptake of Covalent Poly(Allylamine Hydrochloride) Microcapsules and Its Influences on Cell Functions. *Macromol. Biosci.* **2012**, *12*, 1534-1545.

View Article Online
DOI: 10.1039/C7CP07353D

34. Cranford, S. W.; Ortiz, C.; Buehler, M. J., Mechanomutable Properties of a Paa/Pah Polyelectrolyte Complex: Rate Dependence and Ionization Effects on Tunable Adhesion Strength. *Soft Matter* **2010**, *6*, 4175-4188.
35. Ferreira, Q.; Gomes, P. J.; Ribeiro, P. A.; Jones, N. C.; Hoffmann, S. V.; Mason, N. J.; Oliveira, O. N.; Raposo, M., Determination of Degree of Ionization of Poly(Allylamine Hydrochloride) (Pah) and Poly 1- 4-(3-Carboxy-4 Hydroxyphenylazo)Benzene Sulfonamido - 1,2-Ethanediyl, Sodium Salt (Pazo) in Layer-by-Layer Films Using Vacuum Photoabsorption Spectroscopy. *Langmuir* **2013**, *29*, 448-455.
36. Troiano, J. M., et al., Quantifying the Electrostatics of Polycation–Lipid Bilayer Interactions. *Journal of the American Chemical Society* **2017**.
37. Kondinskaia, D. A.; Kostritskii, A. Y.; Nesterenko, A. M.; Antipina, A. Y.; Gurtovenko, A. A., Atomic-Scale Molecular Dynamics Simulations of DNA-Polycation Complexes: Two Distinct Binding Patterns. *Journal of Physical Chemistry B* **2016**, *120*, 6546-6554.
38. Palermo, E. F.; Kuroda, K., Chemical Structure of Cationic Groups in Amphiphilic Polymethacrylates Modulates the Antimicrobial and Hemolytic Activities. *Biomacromolecules* **2009**, *10*, 1416-1428.
39. Mecke, A.; Majoros, I. J.; Patri, A. K.; Baker, J. R.; Holl, M. M. B.; Orr, B. G., Lipid Bilayer Disruption by Polycationic Polymers: The Roles of Size and Chemical Functional Group. *Langmuir* **2005**, *21*, 10348-10354.
40. Diamanti, E.; Andreozzi, P.; Anguiano, R.; Yate, L.; Gregurec, D.; Politakos, N.; Ziolo, R. F.; Donath, E.; Moya, S. E., The Effect of Top-Layer Chemistry on the Formation of Supported Lipid Bilayers on Polyelectrolyte Multilayers: Primary Versus Quaternary Amines. *Physical Chemistry Chemical Physics* **2016**, *18*, 32396-32405.
41. Ohno, P. E.; Saslow, S. A.; Wang, H.-f.; Geiger, F. M.; Eisenthal, K. B., Phase-Referenced Nonlinear Spectroscopy of the Alpha-Quartz/Water Interface. *Nature communications* **2016**, *7*, 13587.
42. Troiano, J. M., et al., Direct Probes of 4 Nm Diameter Gold Nanoparticles Interacting with Supported Lipid Bilayers. *The Journal of Physical Chemistry C* **2015**, *119* 534-546.
43. Troiano, J. M.; Kuech, T. R.; Vartanian, A. M.; Torelli, M. D.; Sen, A.; Jacob, L. M.; Hamers, R. J.; Murphy, C. J.; Pedersen, J. A.; Geiger, F. M., On Electronic and Charge Interference in Second Harmonic Generation Responses from Gold Metal Nanoparticles at Supported Lipid Bilayers. *The Journal of Physical Chemistry C* **2016**, *120*, 20659-20667.
44. McGeachy, A. C.; Olenick, L. L.; Troiano, J. M.; Lankone, R. S.; Melby, E. S.; Kuech, T. R.; Ehimiaghe, E.; Fairbrother, D. H.; Pedersen, J. A.; Geiger, F. M., Resonantly Enhanced Nonlinear Optical Probes of Oxidized Multiwalled Carbon Nanotubes at Supported Lipid Bilayers. *The Journal of Physical Chemistry B* **2017**, *121*, 1321-1329.
45. Olenick, L. L.; Chase, H. M.; Fu, L.; Zhang, Y.; McGeachy, A. C.; Dogangun, M.; Walter, S. R.; Wang, H.-f.; Geiger, F. M., Single-Component Supported Lipid Bilayers Probed Using Broadband Nonlinear Optics. *Physical Chemistry Chemical Physics* **2017**.
46. Anderson, T. H.; Min, Y.; Weirich, K. L.; Zeng, H.; Fygenson, D.; Israelachvili, J. N., Formation of Supported Bilayers on Silica Substrates. *Langmuir* **2009**, *25*, 6997-7005.
47. Rao, Y.; Kwok, S. J. J.; Lombardi, J.; Turro, N. J.; Eisenthal, K. B., Label-Free Probe of Hiv-1 Tat Peptide Binding to Mimetic Membranes. *Proceedings of the National Academy of Sciences of the United States of America* **2014**, *111*, 12684-12688.
48. Ohno, P. E.; Wang, H.-f.; Geiger, F. M., Second-Order Spectral Lineshapes from Charged Interfaces, in Press. *Nature communications* **2017**, *arXiv, 1703.03686*.

View Article Online
DOI: 10.1039/C7CP07353D

49. Boamah, M. D.; Ohno, P. E.; Geiger, F. M.; Eisenthal, K. B., Relative Permittivity in the Electrical Double Layer from Nonlinear Optics. *arXiv 1702.02496 and in press at J. Chem. Phys. (2018)* **2017**.
50. Wang, H.; Yan, E. C. Y.; Borguet, E.; Eisenthal, K. B., Second Harmonic Generation from the Surface of Centrosymmetric Particles in Bulk Solution. *Chemical Physics Letters* **1996**, *259*, 15-20.
51. Liu, Y.; Yan, C. Y.; Zhao, X. L.; Eisenthal, K. B., Surface Potential of Charged Liposomes Determined by Second Harmonic Generation. *Langmuir* **2001**, *17*, 2063-2066.
52. Gonella, G.; Lutgebaucks, C.; de Beer, A. G. F.; Roke, S., Second Harmonic and Sum-Frequency Generation from Aqueous Interfaces Is Modulated by Interference. *Journal of Physical Chemistry C* **2016**, *120*, 9165-9173.
53. Hayes, P. L.; Malin, J. N.; Jordan, D. S.; Geiger, F. M., Get Charged Up: Nonlinear Optical Voltammetry for Quantifying the Thermodynamics and Electrostatics of Metal Cations at Aqueous/Oxide Interfaces. *Chemical Physics Letters* **2010**, *499*, 183-192.
54. Malin, J. N.; Hayes, P. L.; Geiger, F. M., Interactions of Ca, Zn, and Cd Ions at Buried Solid/Water Interfaces Studied by Second Harmonic Generation. *Journal of Physical Chemistry C* **2009**, *113*, 2041-2052.
55. Langmuir, I., The Constitution and Fundamental Properties of Solids and Liquids Part I Solids. *Journal of the American Chemical Society* **1916**, *38*, 2221-2295.
56. Masel, R. I., *Principles of Adsorption and Reaction on Solid Surfaces*; Wiley: New York [u.a.], 1996.
57. Barcroft, J.; Hill, A. V., The Nature of Oxyh Ae Moglobin, with a Note on Its Molecular Weight. *Journal of Physiology-London* **1910**, *39*, 411-428.
58. Mosior, M.; McLaughlin, S., Electrostatics and Reduction of Dimensionality Produce Apparent Cooperativity When Basic Peptides Bind to Acidic Lipids in Membranes. *Biochimica Et Biophysica Acta* **1992**, *1105*, 185-187.
59. Torrens, F.; Castellano, G.; Campos, A.; Abad, C., Negatively Cooperative Binding of Melittin to Neutral Phospholipid Vesicles. *Journal of Molecular Structure* **2007**, *834*, 216-228.
60. Solomatin, S. V.; Greenfeld, M.; Herschlag, D., Implications of Molecular Heterogeneity for the Cooperativity of Biological Macromolecules. *Nature Structural & Molecular Biology* **2011**, *18*, 732-734.
61. Mosior, M.; McLaughlin, S., Binding of Basic Peptides to Acidic Lipids in Membranes. *Faseb J.* **1992**, *6*, A88-A88.
62. Kim, J. Y.; Mosior, M.; Chung, L. A.; Wu, H.; McLaughlin, S., Binding of Peptides with Basic Residues to Membranes Containing Acidic Phospholipids. *Biophysical Journal* **1991**, *60*, 135-148.
63. Pelton, R., Polyvinylamine: A Tool for Engineering Interfaces. *Langmuir* **2014**, *30*, 15373-15382.
64. Sander, M.; Tomaszewski, J. E.; Madliger, M.; Schwarzenbach, R. P., Adsorption of Insecticidal Cry1ab Protein to Humic Substances. 1. Experimental Approach and Mechanistic Aspects. *Environmental Science & Technology* **2012**, *46*, 9923-9931.
65. Katchalsky, A.; Mazur, J.; Spitnik, P., Polybase Properties of Polyvinylamine. *Journal of Polymer Science* **1957**, *23*, 513-532.
66. Westman, E. H.; Ek, M.; Enarsson, L. E.; Wagberg, L., Assessment of Antibacterial Properties of Polyvinylamine (Pvam) with Different Charge Densities and Hydrophobic Modifications. *Biomacromolecules* **2009**, *10*, 1478-1483.

View Article Online
DOI: 10.1039/C7CP07353D

67. Theato, P.; Zentel, R., Formation of Lipid Bilayers on a New Amphiphilic Polymer Support. *Langmuir* **2000**, *16*, 1801-1805.
68. Zhang, L. Q.; Longo, M. L.; Stroeve, P., Mobile Phospholipid Bilayers on a Polyion/Alkylthiol Layer Pair. *Langmuir* **2000**, *16*, 5093-5099.
69. Shao, J. X.; Wen, C. X.; Xuan, M. J.; Zhang, H. Y.; Frueh, J.; Wan, M. W.; Gao, L. H.; He, Q., Polyelectrolyte Multilayer-Cushioned Fluid Lipid Bilayers: A Parachute Model. *Physical Chemistry Chemical Physics* **2017**, *19*, 2008-2016.
70. Volden, S.; Genzer, J.; Zhu, K. Z.; Ese, M. H. G.; Nystrom, B.; Glomm, W. R., Charge- and Temperature-Dependent Interactions between Anionic Poly (N-Isopropylacrylamide) Polymers in Solution and a Cationic Surfactant at the Water/Air Interface. *Soft Matter* **2011**, *7*, 8498-8507.
71. Delajon, C.; Gutberlet, T.; Steitz, R.; Mohwald, H.; Krastev, R., Formation of Poly,Electrolyte Multilayer Architectures with Embedded Dmpc Studied in Situ by Neutron Reflectometry. *Langmuir* **2005**, *21*, 8509-8514.

Figure Captions.

Figure 1. Structures of the polycations studies herein: (a) poly(diallyldimethly amamonium chloride) (PDADMAC), (b) poly(vinylamine hydrochloride) (PVAm), (c) poly-L-lysine hydrobromide (PLL), and (d) poly-L-arginine hydrochloride (PLR).

Figure 2. Normalized SHG *E*-field as a function of time in the presence SLBs formed from (a) DMPC or (b) 9:1 DMPC/DMPG for 50 nM $PDADMAC_{400}$ (dark purple), 50 nM $PDADMAC_{100}$ (light purple), 500 nM PLL (light green), 500 nM PLR (red), and 50 nM PVAm (teal) at 0.1 M NaCl, 0.01 M Tris, pH 7.4. At $t = 0$, the supported lipid bilayer is unperturbed and the SHG

View Article Online
DOI: 10.1039/C7CP07353D

signal is monitored at 0.1 M NaCl. At t = 43 min, polymer solution is introduced into the flow cell and at t = 112 min the flow cell is rinsed with polymer-free solution composed of 0.1 M NaCl, 0.01 M Tris, pH 7.4.

Figure 3. Normalized SHG *E*-field as a function of (a) polymer molar concentration, (b) the number of repeat units (degree of polymerization, DP), in molarity, and (c) amount of positive charge (molar units) at 0.1 M NaCl, 0.01 M Tris, pH 7.4. In (b) the concentration on the basis of repeat units is determined by multiplying the polymer concentration, in molarity, by the number of repeat units. In (c) the concentration of positive charges is determined by multiplying the polymer concentration, in molarity, by the number of repeat units. Each polymer data set is independently normalized and referenced. The SHG *E*-field displayed is normalized to the SHG *E*-field associated with the supported lipid bilayer formed from 9:1 DMPC/DMPG prior to exposure to polymer.

Figure 4. Normalized SHG *E*-field as a function of polymer concentration, in molarity, at 0.1 M NaCl, 0.01 M Tris, pH 7.4 for (a) $PDADMAC_{400}$, (b) $PDADMAC_{100}$, (c) PVAm, (d) PLL, and (e) PLR. SHG *E*-field is normalized to the SHG *E*-field associated with the supported lipid bilayer formed from 9:1 DMPC/DMPG prior to exposure to polymer. Each individual adsorption isotherm is shown with the corresponding fit with the combined Hill/Gouy-Chapman equation (black solid line). See main text for further discussion of the model.

View Article Online
DOI: 10.1039/C7CP07353D

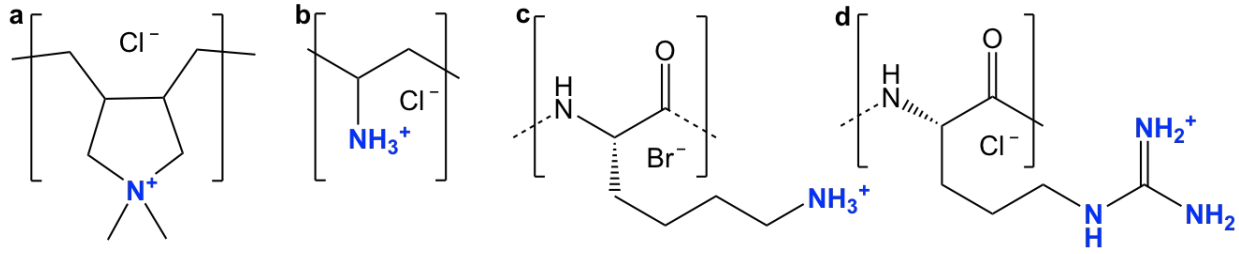

Figure 1.

View Article Online
DOI: 10.1039/C7CP07353D

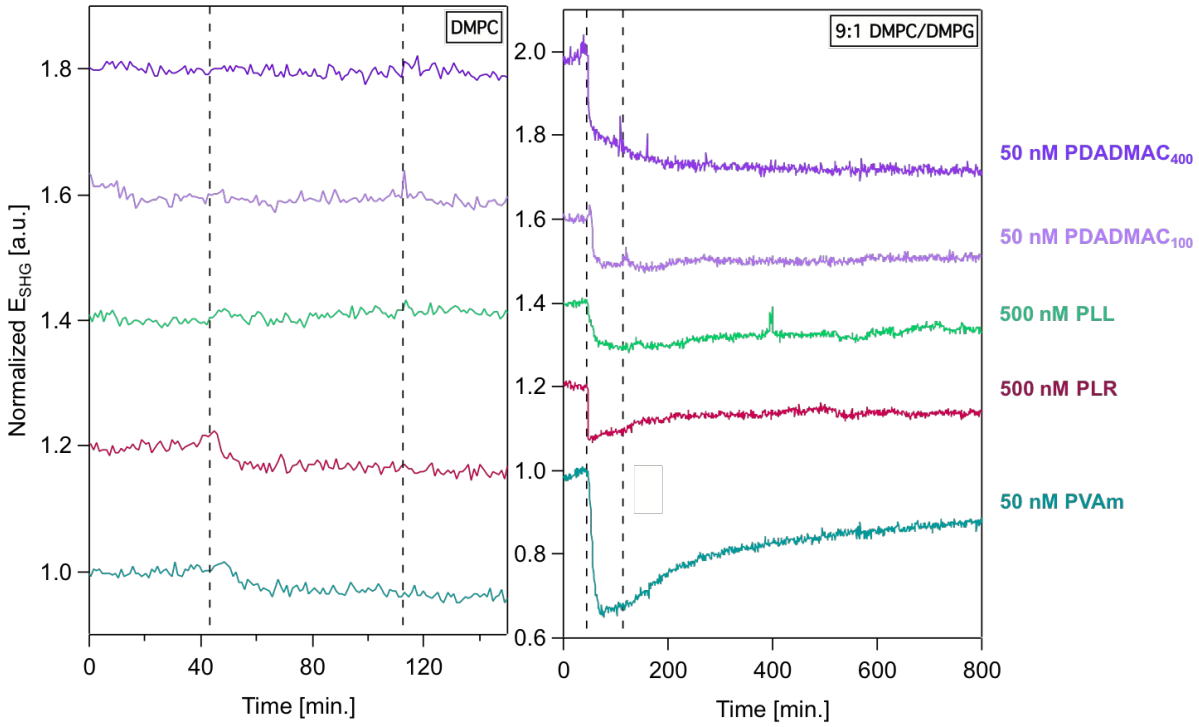

Figure 2.

View Article Online
DOI: 10.1039/C7CP07353D

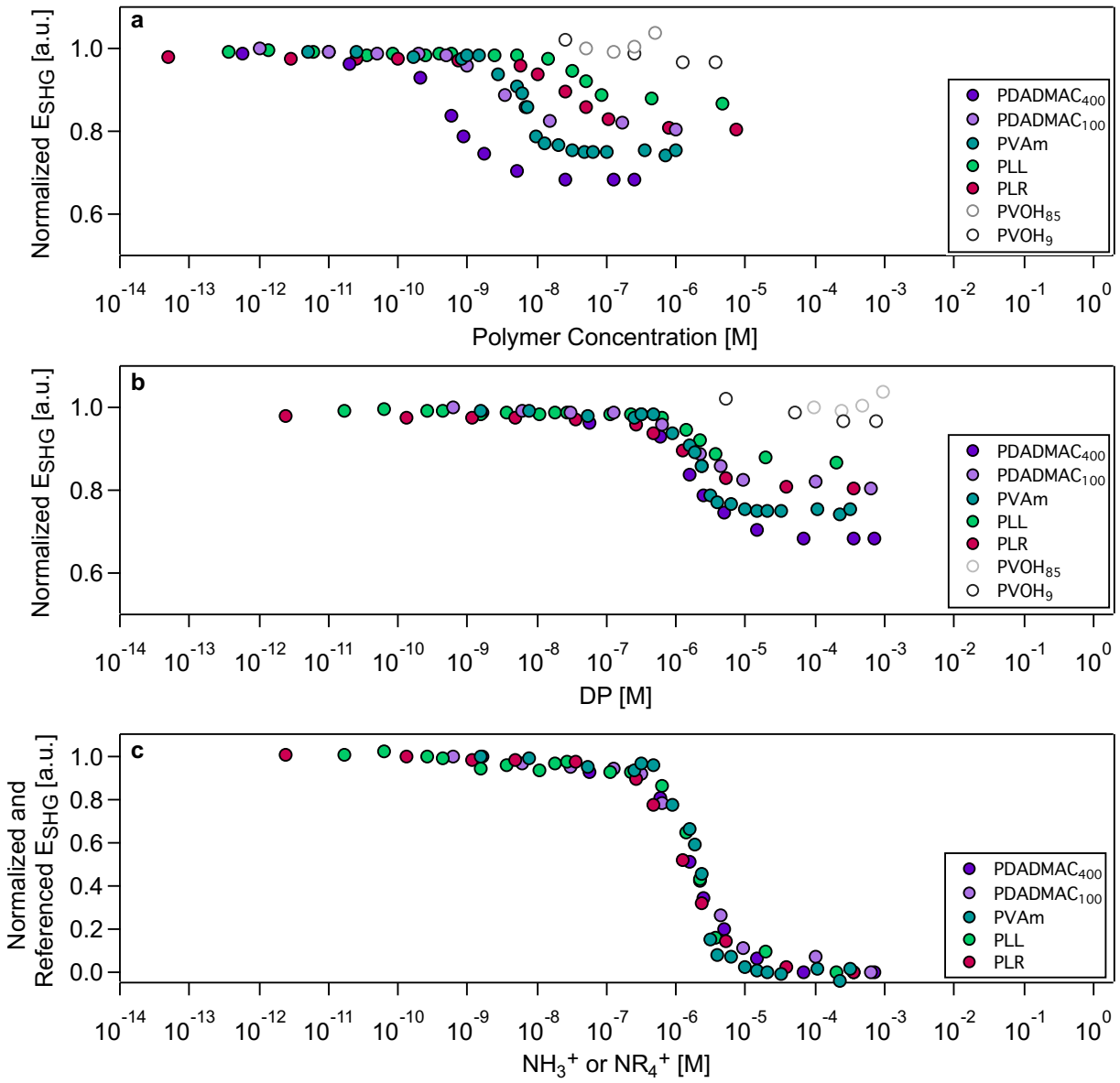

Figure 3.

View Article Online
DOI: 10.1039/C7CP07353D

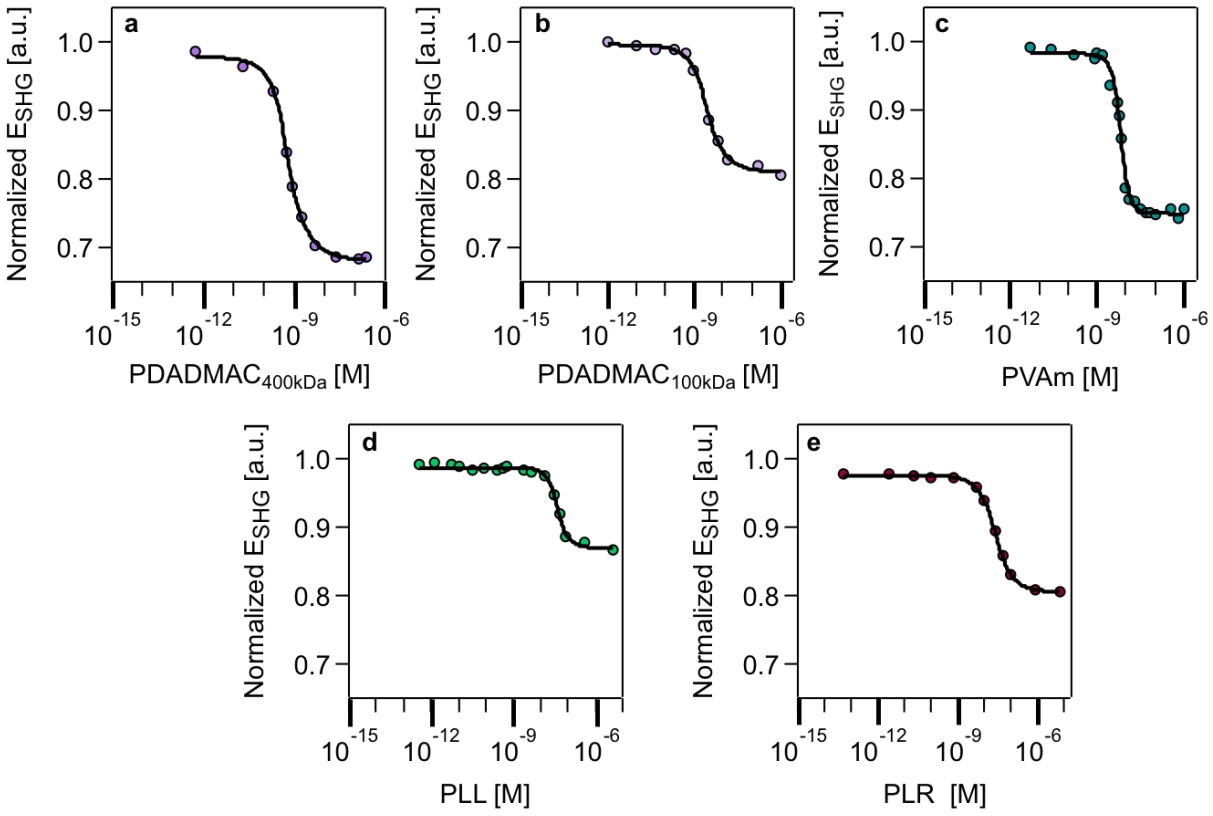

Figure 4.

View Article Online
DOI: 10.1039/C7CP07353D

Table 1. Summary of Experimental Data.

	binding constant	adsorption free energy	surface charge density[a]	Hill coefficient	acoustic surface mass density	number density[b]
	K_{app} [M^{-1}]	ΔG [kJ/mol]	σ [C/m^2]	n	$\Gamma_{QCM\text{-}D}$ [ng/cm^2]	N_{ads} [cm^{-2}]
$PDADMAC_{400}$	$9.5 (\pm 6.1) \times 10^8$	-61 ± 1.6	0.30 ± 0.15	0.93 ± 0.09	260 ± 14	$4.23 (\pm 0.04) \times 10^{11}$
$PDADMAC_{100}$	$2.3 (\pm 2.1) \times 10^8$	-58 ± 2.2	0.27 ± 0.18	0.92 ± 0.14	320 ± 15	$1.22 (\pm 0.07) \times 10^{12}$
PVAm	$1.7 (\pm 0.7) \times 10^8$	-57 ± 1.0	0.16 ± 0.15	2.3 ± 1.0	440 ± 12	$4.48 (\pm 0.2) \times 10^{12}$
PLL	$2.4 (\pm 2.1) \times 10^7$	-52 ± 2.2	0.18 ± 0.20	1.6 ± 0.77	240 ± 12	$1.04 (\pm 0.06) \times 10^{13}$
PLR	$2.8 (\pm 1.4) \times 10^7$	-52 ± 1.2	0.24 ± 0.08	0.89 ± 0.08	220 ± 34	$2.73 (\pm 0.3) \times 10^{12}$

[a]Surface charge density of adsorbed polymer layer (not including charge density of 9:1 DMPC/DMPG bilayer. [b]assuming that 31% of the acoustic surface mass density is attributable to hydrodynamically coupled water.